New Journal of Physics
An Institute of Physics and Deutsche Physikalische Gesellschaft Journal

The dimers stay intact: a quantitative photoelectron study of the adsorption system Si{100}(2x1)-C_2H_4

P Baumgärtel†, R Lindsay†, O Schaff†, T Gießel†, R Terborg†, J T Hoeft†, M Polcik†¶, A M Bradshaw†, M Carbone‡, M N Piancastelli‡, R Zanoni§, R L Toomes‖ and D P Woodruff‖

† Fritz-Haber-Institut der Max-Planck-Gesellschaft, Faradayweg 4-6, 14195 Berlin, Germany
‡ Department of Chemical Sciences and Technologies, University of Roma 'Tor Vergata', 00133 Roma, Italy
§ Department of Chemistry, University of Roma 'La Sapienza', 00185 Roma, Italy
‖ Department of Physics, University of Warwick, Coventry CV4 7AL, UK
E-mail: D.P.Woodruff@Warwick.ac.uk

New Journal of Physics **1** (1999) 20.1–20.15 (http://www.njp.org/)
Received 8 July 1999; online 26 November 1999

Abstract. Using the technique of photoelectron diffraction in the scanned energy mode we show that the Si dimer separation on the Si{100} surface following the adsorption of ethene (ethylene) is $2.36(\pm 0.21)$ Å. This value is only very slightly larger than on the clean surface and shows that the dimer remains intact, thus providing a clear quantitative experimental resolution of a long controversy in the literature. The C–C and C–Si separations are 1.62 ± 0.08 Å and 1.90 ± 0.01 Å, respectively, the former indicating a bond order of less than one.

Contents

¶ Also at: Institute of Physics of the Academy of Science of the Czech Republic, Cukrovarnicka 10, 162 53 Prague, Czech Republic.

1367-2630/99/000020+15$30.00

1. Introduction

While surface reconstruction is now known to be widespread for many clean, single crystal surfaces of semiconductors and metals, silicon surfaces provided some of the very first examples of this phenomenon. Atoms of the outermost layer(s) of a solid take up modified equilibrium positions relative to those of an ideally-truncated bulk crystal which correspond to a configuration of lower surface free energy. The label of 'surface reconstruction' is applied when this involves changes in atomic density or movements parallel (as well as perpendicular) to the surface of at least one atomic layer, leading to a larger surface unit mesh or a lower symmetry. Silicon crystals exposing a $\{100\}$ plane are particularly interesting because this is the normal orientation of the wafer material used in the microelectronics industry. Clean Si$\{100\}$ is reconstructed such that pairs of nearest-neighbour surface Si atoms 'dimerize' to produce ordered structures characterized by (2×1) and c(4×2) unit meshes. (This notation relates the dimensions of the unit cell of the reconstructed surface to that expected from ideal truncation of the bulk structure.) The (2×1) phase was first observed by Schlier and Farnsworth [1] using low energy electron diffraction (LEED) while later temperature-dependent studies showed that this transforms to the c(4×2) phase at low temperature [2]. The thermal behaviour is important since the dimers are actually asymmetric, or buckled (i.e. the Si–Si bond is inclined relative to the surface plane). Below $\sim$200 K these asymmetric dimers order to form two domains of a c(4×2) structure consisting of alternately inclined Si–Si bonds, a model first proposed by Chadi [3]. Above this temperature this asymmetry ordering is lost and the dimers 'flip' rapidly between the two symmetrically equivalent forms, giving rise to the observed average (2×1) periodicity (also in two domains). Scanning tunnelling microscope (STM) images are consistent with this behaviour [4, 5].

In a simple picture dimer formation occurs in order to decrease from two to one the number of dangling bonds (i.e. unsaturated hybridized valence orbitals created by the surface truncation) per Si atom. In the past few years attention has focussed on the adsorption of small, unsaturated hydrocarbon molecules on Si$\{100\}$ [6] and is motivated by the requirement to anchor ultra-thin organic layers to this surface for use in sensors or even in future nanometer-scale integrated circuitry ('molecular electronics'). Olefinic and acetylenic hydrocarbons (>C=C< and -C≡C-, respectively) form relatively stable bonds to the Si$\{100\}$ surface by bonding along the dimers in a bridging or so-called di-σ configuration, thereby saturating the remaining dangling bonds. This adsorption geometry is shown schematically in figure 1 in which the dimers are assumed to be symmetric, as might occur in the presence of the adsorbate. Qualitative support for this general bonding picture comes from a range of investigations in the last few years using various surface spectroscopies [7]–[21] including a very recent Si 2p high-resolution core-level-shift analysis [22]. A major controversy, however, has surrounded the structure of such a passivated surface. Does the Si–Si dimer bond remain intact [6]–[8], [21] on adsorption of ethene (ethylene) and ethyne (acetylene), or is there a cleavage of the dimer with 'insertion' of the adsorbate into the Si–Si bond [11]–[17]? Recent *ab initio* calculations [23]–[27] actually indicate that the Si–Si bondlength remains essentially unchanged. Moreover, the measured photoemission spectrum has been found to be consistent with the Kohn–Sham one-particle energies calculated by Widdra *et al*

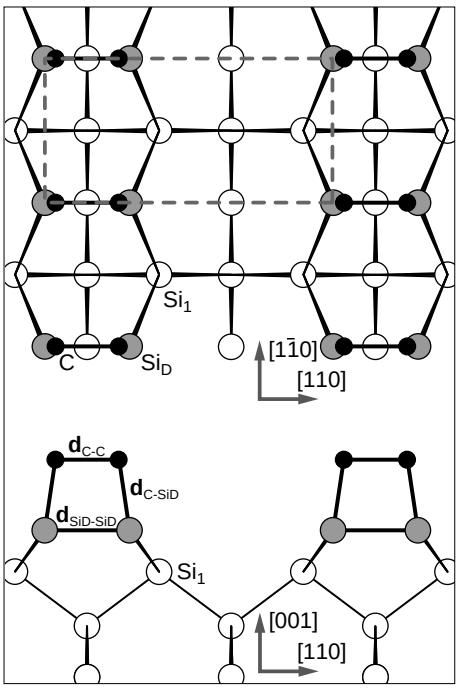

Figure 1. Schematic plan and side views of a Si(100)(2×1) surface with symmetric surface dimers and ethene adsorbed symmetrically above these dimers. The main structural parameters of this model are labelled. The dashed line shows the (2×1) unit mesh.

[20] and Birkenheimer *et al* [27]. Various semi-empirical calculations have also been performed [28]–[33]; one, [31], favoured the dimer-cleaved structure, whereas two others [28, 29] supported the notion of intact dimers. A recent discussion of this issue [34], including discussion of detailed STM studies, concluded that the dimer bond is not broken, but this conclusion relies heavily on the results of the theoretical studies. So far, no quantitative experimental structural investigation has been performed.

We report here a study of the Si$\{100\}(2 \times 1)$-C_2H_4 system using photoelectron diffraction in the scanned energy mode. In this technique the intensity of a core level photoemission line from an atom of the adsorbate is measured at a fixed emission angle as a function of photon energy, and thus of photoelectron kinetic energy [35]. Synchrotron radiation is clearly necessary for this experiment. The intensity is dependent—amongst other parameters—on the elastic scattering of the photoelectron wave at the surrounding (substrate) atoms in the final state. That part of the photoelectric wavefield which reaches the detector directly through the vacuum half-space will combine coherently at the detector with those parts resulting from the various elastic scattering events. Since the path-length differences depend on the coordinates of the emitter atom relative to the neighbouring substrate atoms, the resulting intensity modulations as a function of photoelectron kinetic energy will contain structural information. This is extracted by comparing such data for several different emission angles with simulated modulation functions which are calculated for various model structures using suitable computer codes which explicitly include multiple scattering. In recent years we have shown that the techniques can be applied successively to many molecular adsorbates, including hydrocarbons, e.g. [36, 37], on metal surfaces, and have

recently also demonstrated its potential for studies of adsorbates at silicon surfaces [38]–[40]. We show here that the Si–Si dimer on the $\{100\}$ face does indeed remain intact upon adsorption of ethene and appears to adopt a symmetric geometry in the presence of this adsorbate.

2. Experimental details

The experiments were conducted at the BESSY I synchrotron radiation facility in Berlin on the HE-TGM-1 beam line [41]. The purpose-built UHV chamber is equipped with sample heating and cooling facilities, LEED optics and a concentric spherical sector electron spectrometer (VG Scientific, 152 mm radius, three channeltron detector) for soft x-ray photoelectron spectroscopy (SXPS). The latter allows the characterization of surface cleanness as well as the measurement of the photoelectron diffraction spectra themselves. The Si$\{100\}$ 0.5 mm thick wafer (P doped, 10 Ω cm) cleaved to a rectangle of 12 mm $\times$ 7 mm was cleaned *ex situ* by rinsing in methanol and ultra-pure water and mounted on the UHV manipulator with the capability for direct current heating together with cooling from a liquid helium reservoir connected by copper braid to one of the metal clips of the sample mounting. *In situ* cleaning was achieved by flashing to 1520 K to yield a surface showing a well-ordered two-domain (2×1) LEED pattern at room temperature with no detectable contamination seen in the SXPS data. All measurements were made with the sample cooled with liquid helium; the temperature reading at the metallic clip holding the sample was typically 60 K, although the true sample temperature is likely to be higher than this; the observation of the two-domain c(4×2) LEED pattern for the clean surface clearly indicates the sample temperature was below about 200 K [2], and probably substantially lower.

The sample was exposed at low temperature to 2×10^{-5} mbar s of ethene, which was established, on the basis of the C 1s peak intensity in SXPS after successive doses, to correspond to a saturation coverage. Following this exposure the LEED pattern changed to one characteristic of two orthogonal domains of a (2×1) unit mesh. This behaviour has been interpreted in terms of ethene removing the asymmetry of the alternately inclined dimers, such that the Si–Si axes become parallel to the surface, which gives rise to the smaller unit mesh [7]–[21]. Asymmetric dimers can of course also give rise to a (2×1) structure, but must be all inclined in the same direction (or have a random arrangement of asymmetry tilts to give an average (2×1) periodicity). Clearly, this possibility might have to be checked in the simulation of the photoelectron diffraction data.

The C 1s photoelectron diffraction data were measured in the kinetic energy range 100–470 eV in the two main azimuthal directions $\langle 100 \rangle$ and $\langle 110 \rangle$ for polar emission angles between 0° and 60° in steps of 10° with additional measurements at 15°. The signal was recorded at successive photon energies (separated by 2 eV) in the kinetic energy range of ± 25 eV around the C 1s core level peak to give a series of energy distribution curves (EDCs). The intensity of the peak in each EDC was then determined by background subtraction and integration, and the resulting intensity-energy spectra were normalized to give the photoelectron diffraction modulation functions. The modulation function is defined by

$$\chi_{ex}(\theta, \phi, k) = (I(k) - I_0(k))/I_0(k) \tag{1}$$

where $I(k)$ and $I_0(k)$ are the diffractive and non-diffractive intensities, θ and ϕ are the polar and azimuthal emission angles and k is the modulus of the photoelectron wave vector. $I_0(k)$ is obtained by performing a smooth fit to $I(k)$ with a spline function (assuming that the non-diffractive part of the intensity changes only slowly as a function of energy). Nine such

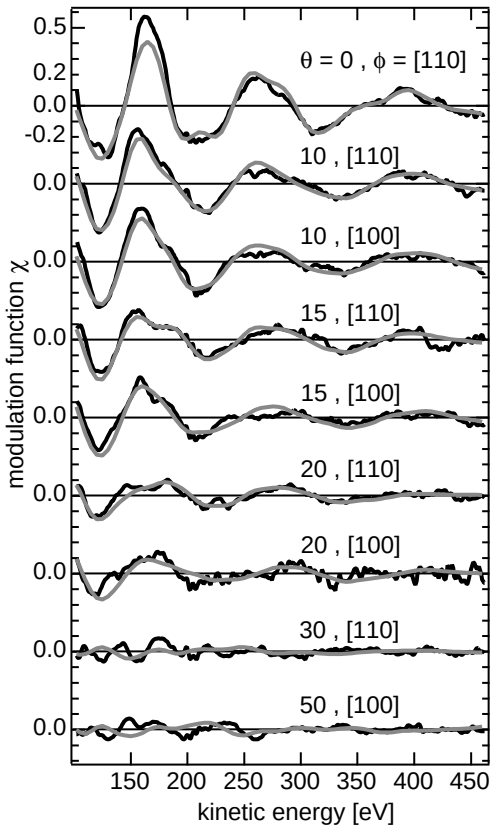

Figure 2. Experimental C 1s photoelectron diffraction modulation spectra (bold lines) recorded from the Si(100)(2×1)-C_2H_4 surface in various emission geometries compared with the results of the calculations (grey lines) for the best-fit structure.

modulation functions were selected for the full quantitative structure optimization described in the next section; these are shown as the bold curves in figure 2.

3. Data analysis and the multiple scattering calculations

Quantitative information on the local geometry of the emitter atom is extracted in a similar way to the method used in LEED by comparing experimental modulation functions measured at several different emission angles with simulated curves calculated using multiple scattering theory. Our 'integrated approach' to photoelectron diffraction structure determination generally proceeds in two stages [35]. A direct method is first used to determine the adsorption site in which the full set, or a sub-set, of the data is employed to calculate the so-called projection integrals [42]. The underlying physical principle is that modulation functions measured in directions which correspond to 180° scattering from a near-neighbour substrate atom ('the backscattering geometry') are typically dominated by this event and show particularly strong intensity modulations. This modulation function can thus be described reasonably well within the single scattering approximation with only one scatterer taken into account. The method therefore involves the calculation of integrals of the actual experimental spectra projected

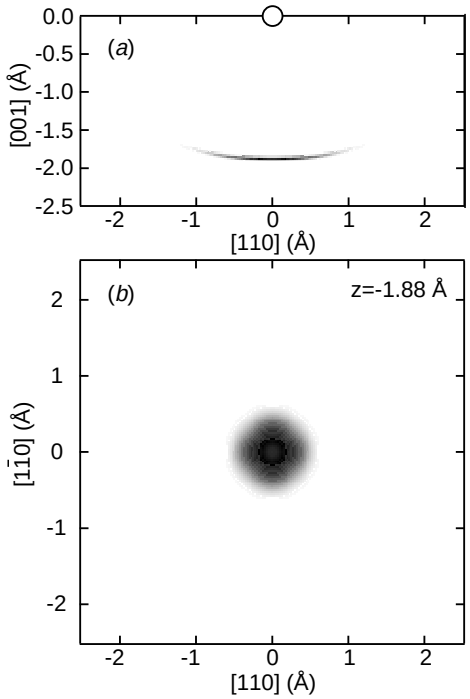

Figure 3. Results of applying the projection method of direct data inversion to the experimental photoelectron diffraction spectra of figure 2. The projection method provides a three-dimensional 'image' of the surroundings of the emitter (located at (0, 0, 0)), the parameter mapped having the highest intensity at locations most likely to correspond to those of near-neighbour backscatterers. (*a*) shows a grey-scale mapping of this parameter in a plane perpendicular to the surface passing through the emitter in a $\langle 110 \rangle$ azimuth. (*b*) shows a similar mapping in a plane parallel to the surface and 1.88 Å below the emitter.

onto such calculated spectra based on this simple single scattering description and produces a three-dimensional intensity map of the space around the emitter, with maximum values of the projection integral in regions corresponding to the most probable locations of nearest neighbour backscatterers.

The second stage is a full quantitative structural analysis using an iterative 'trial-and-error' procedure which involves a comparison of usually 5–10 experimental spectra with the results of multiple scattering simulations based on trial model structures. These calculations are performed with codes developed by Fritzsche [43, 44] which are based on the expansion of the final state wave-function into a sum over all scattering pathways which the electron can take from the emitter atom to the detector outside the sample. A magnetic quantum number expansion of the free electron propagator is used to calculate the scattering contribution of an individual scattering path. Double and higher order scattering events are treated by means of the reduced angular momentum expansion (RAME). The finite energy resolution and angular acceptance of the electron analyser are included. Anisotropic vibrations for the emitter atom and isotropic vibrations for the scattering atoms are also taken into account. The comparison between theory

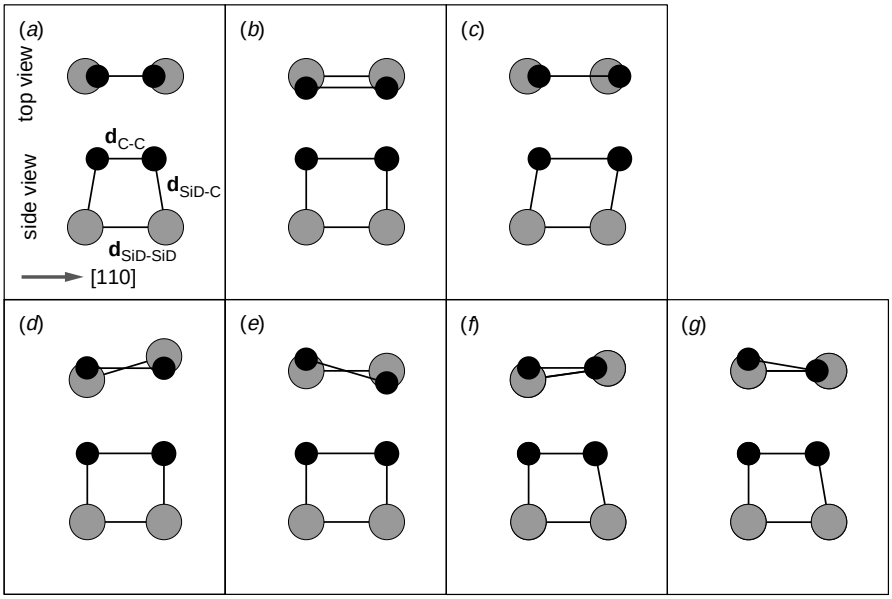

Figure 4. Schematic top and side views of a series of ethene adsorption geometries on a Si dimer on a Si(100) surface which could be compatible with all C atoms being offset by a nominal 0.3 Å from atop the Si atoms in the $\langle 110 \rangle$ azimuths. In all cases the Si dimer bondlength has been set at the clean surface value of 2.29 Å. As discussed in the text, only the model (*a*) leads to a plausible C–C bondlength.

and experiment is aided by the use of a reliability factor

$$R_m = \sum(\chi_{th} - \chi_{ex})^2 / \sum(\chi_{th}^2 + \chi_{ex}^2) \tag{2}$$

where a value of 0 corresponds to perfect agreement, a value of 1 to uncorrelated data, and a value of 2 to anti-correlated data. The search in parameter space to locate the structure having the minimum R-factor was performed with the help of an adapted Newton–Gauss algorithm and an approximate 'linear' version of the multiple scattering code in the initial searches [45]. In order to estimate the errors associated with the individual structural parameters we use an approach based on that of Pendry which was derived for LEED [46]. This involves defining a variance in the minimum of the R-factor, R_{min} as

$$Var = R_{min}\sqrt{2/N} \tag{3}$$

where N is the number of independent pieces of structural information contained in the set of modulation functions used in the analysis. All parameter values giving structures with R-factors less than $R_{min} + Var(R_{min})$ are regarded as falling within one standard deviation of the 'best fit' structure. More details of this approach, in particular on the definition of N, can be found in a recent publication [47]. Note that the precision in individual parameters is usually determined by investigating the change in R_m with this parameter alone, and approach which neglects any possible role of coupling between two or more parameters. In the present case checks revealed there were no instances of strong coupling of this kind.

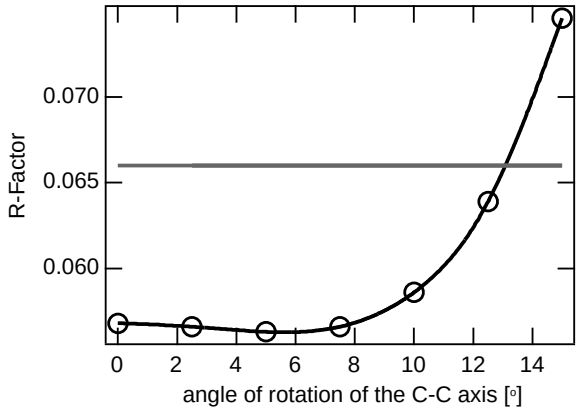

Figure 5. Dependence of the R-factor for the theory/experiment comparison on the presence of an azimuthal twist of the C–C axis of the ethene molecule out of the $\langle 110 \rangle$ symmetry direction. Note that the twist has been performed at a constant value of $d_{\mathrm{SiD-C}}$. The horizontal line corresponds to an R-value equal to the sum of the minimum and its variance, which therefore defines the formal limits of precision.

4. Results and discussion

From the experimental C1s modulation functions in figure 2 it is immediately obvious that the modulations at 0° have the highest amplitude, but decay so quickly with emission angle that already at 30° they are comparable in magnitude to the noise level. Moreover, the modulation functions up to 20° are dominated by a single strong oscillation. This is a clear indication that one, and most probably both, of the C atoms are adsorbed either directly atop, or nearly atop substrate Si atoms. As explained in section 3, normal emission then corresponds to the favoured 180° back-scattering configuration for which there is a maximum in the modulus of the scattering cross-section (as a function of scattering angle). The modulations are strongly damped in off-normal emission directions due to the presence of strongly anisotropic vibrational amplitudes. The frustrated translational and rotational motions parallel to the surface tend to have much higher amplitudes than those perpendicular to the surface when an atop site, as opposed to the hollow site, is occupied. A similar result has been obtained for the adsorption of ethene on Ni$\{111\}$ [48], where the molecule adsorbs in an aligned bridge geometry such that the two C atoms lie close to atop, and also for other adsorbates such as CO [49], PF_3 [50] and NH_3 [47] which adopt atop adsorption sites. It should be noted that the modulation functions in figure 2 also contain subsidiary maxima which do not correspond to the dominant oscillation e.g. at 270 eV for $\theta = 0°$ and at 180 eV for $\theta = 10°$, $15°$ and $20°$, highlighting the fact that the spectra are not only influenced by the nearest neighbour backscatterers.

The result of the application of the projection method to the data of figure 2 is shown in figure 3. The grey-scale plots are sections of real space around the emitting C atom in which the darkest regions correspond to the most likely positions of the nearest neighbour Si atoms. Figure 3(*a*) represents a section perpendicular to the surface through the C atom in the $\langle 110 \rangle$ azimuth and shows a dark streak centred approximately 1.90 Å immediately below the emitter. Another cut *parallel* to the surface 1.88 Å below the emitter, i.e. at the position of the dark streak,

is shown in figure 3(*b*). This intensity pattern indicates, in agreement with the conclusions from the visual inspection of the modulation function in the previous paragraph, that the Si atoms are directly or almost directly below the emitter, i.e. the C atoms occupy atop or near atop sites. The saucer-like form of the image is typical for the projection method and is due to the fact that the features mapped are due to the intersections of surfaces of constant scattering path-length difference, typically paraboloids around the emitter. We note that the saucer-shaped feature does not exhibit its highest intensity in its centre, but in a ring around the centre. While the projection method is not intended to give precise structural positions, this characteristic of the image of figure 3(*b*) may indeed be indicative of a near-atop, rather than exact atop, geometry. The highest intensities are actually in four symmetrically-equivalent positions in this ring offset in the $\langle 110 \rangle$ azimuths, the four-fold symmetry of the pattern deriving from the presence of the two orthogonal domains of the (2×1) structure.

The idea behind the projection method (as in any direct method in crystallography) is to obtain an approximate solution and thus to reduce considerably the size of the parameter space to be explored in the trial-and-error analysis which is the basis of the actual quantitative structural determination. In the present case, the parameter space is particularly large because of the several degrees of freedom associated not only with the C atoms but also with the Si atoms forming the dimer. Fortunately, the projection method tells us very clearly that the C atoms are in atop, or near atop, sites and that they are (locally) equivalent. In addition, we know from spectroscopy [7]–[21] that the ethene retains its molecular integrity, although some considerable distortion, in particular C–C bond lengthening and a 'bending-up' of the hydrogen atoms, might be expected. The equivalent C atoms also mean that the C–C bond, to within the approximation allowed by the direct method, is parallel to the surface. This information strongly indicates that a structure very similar to figure 1 (or figure 4(*a*)) must pertain, i.e. one in which the dimers are more or less 'intact'. A typical Si–Si dimer length on the clean surface is 2.29 Å [51], similar to the bulk Si–Si nearest neighbour distance of 2.36 Å, while it is unreasonable to expect that the C–C bond in adsorbed ethene is longer than about 1.7 Å, so this geometry places the C atoms about 0.3 Å off atop, broadly consistent with our visual assessment of the photoelectron diffraction data and the mapping given by the projection method. If the Si dimer separation were to be much larger, and especially if it were to approach the Si–Si separation of these same atoms at an ideally-truncated bulk surface (3.84 Å), there is no conceivable geometry in which the C atoms can occupy atop, or near atop, sites and at the same time retaining molecular integrity.

Several other possibilities exist, however, in which the dimers remain intact and the condition of locally equivalent C atoms in off-atop sites is met, as shown in figures 4(*b*)–(*g*), and it is sensible to examine them before proceeding with the full trial-and-error analysis. Figures 4(*b*) and 4(*c*) represent structures where the C–C and Si–Si bondlengths are approximately equivalent. Such adsorption geometries can be immediately eliminated: the clean surface Si dimer bondlength of 2.29 Å is much longer than could correspond to an intact C–C bond (the length of this bond in gas-phase ethane, for example, is 1.54 Å). Figures 4(*d*)–(*g*) show alternative models involving reduced symmetry situations in which the C atoms occupy the same local off-atop geometries but can also lead to C–C bondlengths shorter than the Si dimer length. Models 4(*d*) and 4(*f*) require that the dimers are twisted out of the $\langle 110 \rangle$ azimuths, an unlikely situation since the dimer geometry is determined by the near-sp^3 hybridization at the Si atom which in turn is dictated by bulk bonding; the comparatively weak interaction with the hydrocarbon should not induce a displacive reconstruction. In figure 4(*e*) and 4(*g*) the dimer retains the mirror symmetry, but the ethene molecule adopts a low symmetry site. While the models of figures 4(*f*) and 4(*g*) do

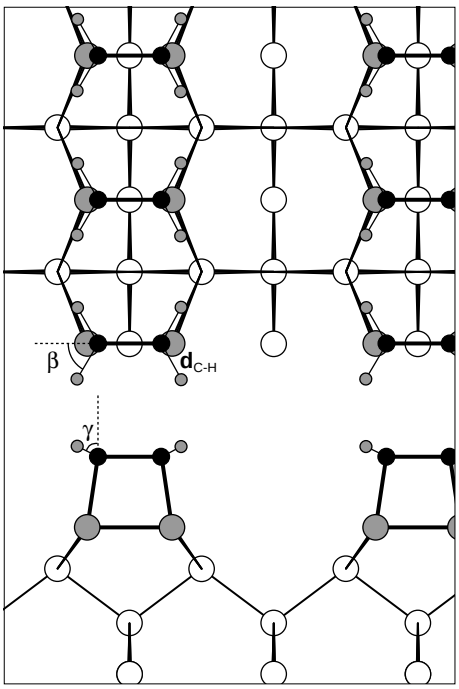

Figure 6. Schematic plan and side views of the Si(100)(2x1)-C_2H_4 adsorption geometry including the H atoms and the definition of the associated angular parameters, β and γ. Note that γ is defined as the angle between the C–H bond and the surface normal, and not the angle to the projection of this bond as it appears in this side view.

lead to C–C bondlengths which are shorter that the Si dimer, reasonable off-atop offsets of 0.3 Å still lead to unacceptably large C–C distances of 1.97 Å and 2.01 Å respectively. In the main quantitative analysis, therefore, only the structure of figure 4(*a*) and minor perturbations from it were considered further.

The starting parameters for the Gauss-Newton optimization of this structural model were $d_{\mathrm{SiD-SiD}} = 2.36$ Å (the bulk Si–Si nearest neighbour distance), $d_{\mathrm{C-SiD}} = 1.88$ Å (implied by the results of the projection method) and a C–C bondlength of 1.45 Å (midway between the values for bond order of two and one). Several simplifying assumptions were made, most of which are intrinsic to the model of figure 4(*a*): the ethene molecule is centred over the dimer with the C–C axis parallel to the surface. The dimer axis is also parallel to the surface and its Si atoms are symmetrically positioned relative to the atoms of the first Si plane in the $\langle 110 \rangle$ azimuths (see figure1). Neither the C–C bond nor the dimer axis were allowed to rotate horizontally or vertically; their centres were also fixed in the mirror planes of the substrate. The parameters varied were thus the C–C bondlength, $d_{\mathrm{C-C}}$, the dimer bondlength $d_{\mathrm{SiD-SiD}}$, the carbon–Si dimer bondlength, $d_{\mathrm{C-SiD}}$, the height of the C atoms relative to the first Si layer, $z_{\mathrm{C-Si1}}$, and their height relative to the Si bulk, $z_{\mathrm{C-SiBulk}}$. The resulting fit gave an R-factor of $R_m = 0.080$ with the mean square vibrational amplitudes of both the Si and C atoms fixed at 0.003 Å^2, the value expected for bulk Si atoms on the basis of the known Debye temperature. The final analysis included a fit of both the mean square amplitudes of vibration and the muffin tin potential and gave an R-factor of 0.057 with a variance of 0.008. The results are shown in table 1. The R-factors for the individual

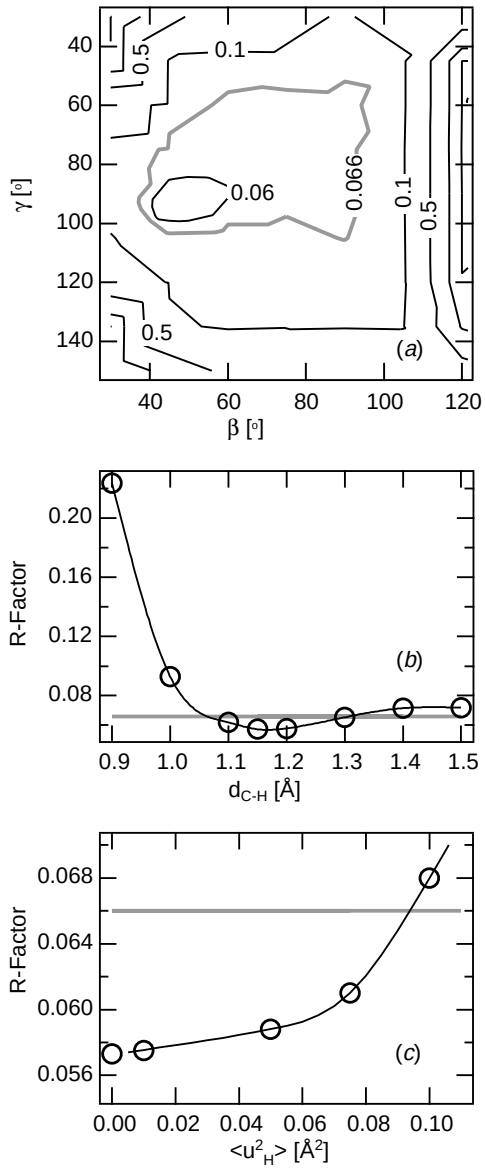

Figure 7. Dependence of the R-factor for the theory/experiment comparison on the parameters associated with the H atom positions. In the upper panel, (*a*), the dependence on both β and γ is shown as a contour map. The grey contour line in this panel, and the horizontal lines in (*b*) and (*c*) correspond to an R-value equal to the sum of the minimum and its variance, which therefore defines the formal limits of precision.

modulation functions in figure 2 (top to bottom) are 0.032, 0.024, 0.030, 0.081, 0.062, 0.167, 0.309, 0.494 and 0.630. The best agreement is of course obtained for those emission angles normal or near-normal to the surface where the modulations are large, and it is these spectra which dominate the global R-factor.

We note that during the optimization the Si dimer separation remains at the starting value of 2.36 Å, but the C–C bondlength increases to 1.62 Å (with a corresponding offset of the C

Table 1. Best-fit structural parameters from this work compared with published theoretical values. Note that the primary structural parameters in PhD are the distances and angles of scatterers relative to the C emitter, so the value of the Si dimer bondlength is derived from the primary parameters of the C–C bondlength, the SiD–C bondlength, and the SiD–C–C bond angle.

	Parameter	This work	Theory [26]	Theory [27]	Theory [25, 34]
Interatomic distances	$d_{\mathrm{C-C}}$	1.62 ± 0.08 Å	1.52 Å	1.50 Å	1.53 Å
	$d_{\mathrm{SiD-SiD}}$	2.36 ± 0.21 Å	2.33 Å	2.39 Å	2.39 Å
	$d_{\mathrm{C-SiD}}$	1.90 ± 0.01 Å	1.93 Å	2.01 Å	1.95 Å
Layer spacings	$z_{\mathrm{C-Si1}}$	2.81 ± 0.18 Å			
	$z_{\mathrm{C-SiBulk}}$	4.41 ± 0.17 Å			
Angle	$\angle \mathrm{SiD-C-C}$	$101.2 \pm 3.0°$	102°	102°	103°
Vibrations	$\langle u^2_{\mathrm{C}} \rangle_{x(\parallel \mathrm{C-C})}$	0.006 ± 0.003 Å^2			
	$\langle u^2_{\mathrm{C}} \rangle_{y(\perp \mathrm{C-C})}$	$0.07 + 0.16/-0.05$ Å^2			
	$\langle u^2_{\mathrm{C}} \rangle_{z}$	0.003 ± 0.002 Å^2			
	$\langle u^2_{\mathrm{SiD}} \rangle$	$0.0003 + 0.0023/-0.0003$ Å^2			
	$\langle u^2_{\mathrm{SiBulk}} \rangle$	$0.0004 + 0.012/-0.0004$ Å^2			
Inner potential		11 ± 5 eV			

atoms from atop of 0.37 Å). The C–C bondlengths in gas-phase ethene and ethane are 1.33 Å and 1.54 Å, respectively, suggesting that the bond here has less than single bond character (although our estimated precision of ± 0.08 Å does lead to the single order bondlength just falling in our acceptable range). The density functional calculations of Pan *et al* [26] and Birkenheuer *et al* [27] give values of 1.52 Å and 1.50 Å, respectively, for the C–C bondlength and 2.33 Å and 2.39 Å, respectively, for the dimer bondlength; Fisher *et al* [25] found a value for the C–C bondlength of 1.53 Å but do not quote the dimer bondlength value (see also table 1). Birkenauer *et al* also found that a slightly lower energy configuration could be obtained by rotating the C–C axis by 11° about the surface normal to give a C_2, as opposed to a C_{2v}, point group. The effect of introducing this parameter as a variable into the present simulations is shown in figure 5. Notice that because the PhD modulations are most sensitive to the distance of the emitter to the nearest-neighbour Si backscatterer, this rotation was accompanied in the calculation by changes in the C–Si layer spacing to maintain a constant value of $d_{\mathrm{SiD-C}}$. The R-factor retains its very low value on rotating the molecule until about 8°, but then rises steeply. The variance in R_{min} is 0.008, so a twist of the C–C axis out of the $\langle 110 \rangle$ azimuth by up to 12° corresponds to the formal error limit. This result was insensitive to whether or not the twisted molecules were ordered in their direction of twist. Notice, however, that the influence of this apparent small static rotation on our data could equally well be assigned to a similar amplitude frustrated rotational vibrational mode of the molecule.

To be absolutely certain that structures eliminated on the basis of the direct method and the comparison with spectroscopy give much higher R-factors, further optimizations were performed for two of the possible alternative models, namely, adsorption on asymmetric dimers and on

cleaved dimers. The starting parameters for the asymmetric dimer optimization were taken from Northrup [51] and the ethene molecule was positioned in corresponding near-atop sites for the C atoms with $d_{C-C} = 1.54$ Å as in the free ethane molecule. The Gauss–Newton optimization gave a local minimum in the R-factor of 0.19 which is much higher than the result above and clearly outside the variance; the associated C–C distance was 1.70 Å which is rather unreasonably large. Similarly, optimizations for a cleaved Si–Si bond and ethene 'insertion' gave no deep local minima and an R-factor always greater than 0.3. It is thus clear that the main question arising from the many experimental studies of this system has been resolved by the present quantitative structural study: the dimer bond very definitely remains intact. Although it is difficult to estimate what the dimer separation would be following cleavage and 'insertion' of the ethene molecule, we note that the separation on a hypothetical surface corresponding to the so-called truncated bulk would be 3.84 Å, which is far outside the margin of error in the present result of $2.36(\pm 0.21)$ Å.

In a short additional study we have also looked at the possibility of gaining any information on the positions of the H atoms, a problem which has so far not been considered in photoelectron diffraction because of the very low scattering cross section for hydrogen. The parameters varied are shown in figure 6 and the corresponding results in figure 7. As expected, the dependence of the R-factor on the two most important parameters, the angles β and γ (the azimuthal and polar angles of the C–H bond relative to the surface normal), is weak and leads to shallow minima, and thus large error bars, with optimum values of $50 + 40/-10°$) and $90 + 12/-40°$, respectively (figure 7(*a*)). Notice, however, that the addition of the H scatterers in these optimum position leads to essentially no change in the minimum R-factor, although, as is shown clearly in figure 7(*a*), putting the H atoms in positions very far from these optimum regions can lead to large increases in the R-factor. In chemical terms, the hybridization at the C atom changes from sp^2 to sp^3 as the C–C bond order is reduced to one (or even less), so the nominal values expected for β and γ (based on the bond angles in ethane and taking no account of the actual value of the C–C–Si bond angle) are $68°$ and $61°$ respectively, both values falling within our (broad) error range. Also shown in figure 7 are the R-factor dependences on the C–H bond length and the mean-square vibrational amplitude of the H atoms. The latter value nominally optimises at zero vibrations, but shows a huge error range, while the C–H bondlength value of 1.18 ± 0.12 Å also encompasses an expected value of around 1.09 Å. Clearly, however, the weakness of the H scattering means that there is no chemically significant information obtained from this analysis regarding the H positions.

5. Conclusions

Using scanned-energy mode photoelectron diffraction we have conducted the first quantitative structural study of the Si(100)(2x1)-C_2H_4 adsorption system, and show clearly that adsorption does not break the Si dimers of the clean surface, but does remove their asymmetry. This provides clear experimental evidence to settle a long-standing controversy as to whether or not the dimers are left intact. Overall this conclusion, and the structural parameters we obtain, are in good agreement with the results of previous *ab initio* theoretical calculations, and especially those of Pan *et al* [26] (see table 1). Our results are consistent with the slight lengthening of the Si dimer from its clean surface value of 2.29 Å [51], indicated by these theoretical studies, although our precision is not quite adequate to exclude an unchanged bondlength. The value for the C–C bondlength we find (1.62 ± 0.08 Å), however, is clearly substantially longer than that in the free molecule (1.33 Å), indicating a significant reduction in the C–C bond order; our value actually

indicates a bond order of *less* than one, although our precision limits include the value of 1.54 Å which is that associated with a single bond and which is also essentially identical to that found in the theoretical studies (see table 1).

Acknowledgments

The authors wish to acknowledge the financial support for this work in the form of grants from the German Federal Ministry of Education, Science, Research and Technology (BMBF—contract number 05 625EBA 6) and the Engineering and Physical Sciences Research Council. AMB and DPW also thank the Max-Planck-Gesellschaft and the Alexander-von-Humbolt-Stiftung for a Max-Planck-Research Prize.

References

[1] Schlier R E and Farnsworth H E 1959 *J. Chem. Phys.* **30** 917
[2] Tabata T, Aruga T and Murata Y 1987 *Surf. Sci.* **179** L63
[3] Chadi D J 1979 *Phys. Rev. Lett.* **43** 43
[4] Hamers R J, Tromp R M and Demuth J E 1986 *Phys. Rev.* B **34** 5343
[5] Wolkow R A 1992 *Phys. Rev. Lett.* **68** 2636
[6] Yates J T Jr 1998 *Science* **279** 335
[7] Nishijima M, Yoshinobu J, Tsuda H and Onchi M 1987 *Surf. Sci.* **192** 383
[8] Yoshinobu J, Tusda H, Onchi M and Nishijama M 1987 *J. Chem. Phys.* **87** 7332
[9] Cheng C C, Wallace R M, Taylor P A, Choyke W J and Yates J T Jr 1990 *Appl. Phys.* **67** 3693
[10] Cheng C C, Choyke W J and Yates J T Jr 1990 *Surf. Sci.* **231** 289
[11] Yates J T Jr 1991 *J. Phys.: Cond. Matt.* **3** S143
[12] Taylor P A, Wallace R M, Cheng C C, Weinberg W H, Dresser M J, Choyke W J and Yates J T Jr 1992 *J. Am. Chem. Soc.* **114** 6754
[13] Clemen L, Wallace R M, Taylor P A, Dresser M J, Choyke W J, Weinberg W H and Yates J T Jr 1992 *Surf. Sci.* bf 268 205
[14] Widdra W, Huang C, Briggs G A D and Weinberg W H 1993 *J. Electron Spectrosc. Relat. Phenom.* **64/65** 129
[15] Huang C, Widdra W, Wang X S and Weinberg W H 1993 *J. Vac. Sci. Technol.* A **11** 2250
[16] Huang C, Widdra W and Weinberg W H 1994 *Surf. Sci.* **315** L953
[17] Widdra W, Huang C and Weinberg W H 1995 *Surf. Sci.* **329** 295
[18] Widdra W, Huang C, Yi S I and Weinberg W H 1996 *J. Chem. Phys.* **105** 5605
[19] Liu H and Hamers R J 1997 *J. Am. Chem. Soc.* **119** 7593
[20] Widdra W, Fink A, Gokhale S, Trischberger P, Menzel D, Birkenheuer U, Gutdeutsch U and Rösch N 1998 *Phys. Rev. Lett.* **80** 4269
[21] Matsui F, Yeom H W, Imanishi A, Isawa K, Matsuda I and Ohta T 1998 *Surf. Sci.* **401** L413
[22] Casaletto M P, Zanoni R, Carbone M, Piancastelli M N, Weiss K and Horn K to be published
[23] Feng K, Liu Z H and Lin Z 1995 *Surf. Sci.* **329** 77
[24] Imamura Y, Morikawa Y, Yamasaki T and Nakatsuji H 1995 *Surf. Sci.* **341** L1091
[25] Fisher A J, Blöchl P E and Briggs G A D 1997 *Surf. Sci.* **374** 298
[26] Pan W, Zhu T and Yang W 1997 *J. Chem. Phys.* **107** 3981
[27] Birkenheuer U, Gutdeutsch U, Rösch N, Fink A, Gokhale S, Menzel D, Trischberger P and Widdra W 1998 *J. Chem. Phys.* **108** 9868
[28] Liu Q and Hoffmann R 1995 *J. Am. Chem. Soc.* **117** 4082
[29] Craig B I and Smith P V 1992 *Surf. Sci.* **276** 174
——1993 *Surf. Sci.* **285** 295

[30] Craig B I 1995 *Surf. Sci.* **329** 293
[31] Carmer C S, Weiner B and Frenklach M 1993 *J. Chem. Phys.* **99** 1356
[32] Zhou R H, Cao P L and Lee L Q 1995 *Phys. Rev.* B **47** 10601
[33] Cao P L and Zhou R H 1993 *J. Phys.: Condens. Matter* **5** 2887
[34] Briggs G A D and Fisher A J 1999 *Surf. Sci. Rep.* **33** 1
[35] Woodruff D P and Bradshaw A M 1994 *Rep. Prog. Phys.* **57** 1029
[36] Schaff O, Stampfl A P J, Hofmann Ph, Bao S, Schindler K-M, Fernandez V, Bradshaw A M, Davis R, Woodruff D P and Fritzsche V 1995 *Surf. Sci.* **343** 201
[37] Schaff O, Fernandez V, Hofmann Ph, Schindler K-M, Theobald A, Fritzsche V, Bradshaw A M, Davis R and Woodruff D P 1996 *Surf. Sci.* **348** 89
[38] Franco N, Avila J, Davila M E, Asensio M C, Woodruff D P, Schaff O, Fernandez V, Schindler K-M, Fritzsche V and Bradshaw A M 1997 *Phys. Rev. Lett.* **79** 673
[39] Franco N, Chrost J, Avila J, Asensio M C, Muller C, Dudzik E, Patchett A J, McGovern I T, Gießel T, Lindsay R, Fritzsche V, Bradshaw A M and Woodruff D P 1998 *Appl. Surf. Sci.* **123** 219
[40] Baumgärtel P, Paggel J J, Hasselblatt M, Horn K, Fernandez V, Schaff O, Weaver J H, Bradshaw A M, Woodruff D P, Rotenberg E and Denlinger J 1999 *Phys. Rev.* B **59** 13014
[41] Dietz E, Braun W, Bradshaw A M and Johnson R 1985 *Nucl. Instrum. Meth.* A **239** 359
[42] Hofmann Ph and Schindler K-M 1993 *Phys. Rev.* B **47** 13941
Hofmann Ph, Schindler K-M, Bao S, Bradshaw A M and Woodruff D P 1994 *Nature* **368** 131
[43] Fritzsche V 1990 *J. Phys.: Condens. Matter* **2** 1413
——1992 *Surf. Sci.* **265** 187
[44] Fritzsche V 1986 *Surf. Sci.* **213** 648
[45] Fritzsche V and Pendry J B 1993 *Phys. Rev.* B **48** 9054
[46] Pendry J B 1980 *J. Phys. C: Solid State Phys.* **13** 937
[47] Booth N A, Davis R, Toomes R, Woodruff D P, Hirschmugl C, Schindler K-M, Schaff O, Fernandez V, Theobald A, Hofmann Ph, Lindsay R, Gießel T and Bradshaw A M 1997 *Surf. Sci.* **387** 152
[48] Bao S, Hofmann Ph, Schindler K-M, Fritzsche V, Bradshaw A M, Woodruff D P, Casado C and Asensio M C 1995 *Surf. Sci.* **323** 19
[49] Hofmann Ph, Schindler K-M, Bao S, Fritzsche V, Bradshaw A M and Woodruff D P 1995 *Surf. Sci.* **337** 169
[50] Dippel R, Weiss K-U, Schindler K-M, Gardner P, Fritzsche V, Bradshaw A M, Asensio M C, Hu X M, Woodruff D P and Gonzalez-Elipe A R 1992 *Chem. Phys. Lett.* **199** 625
[51] Northrup J E 1993 *Phys. Rev.* B **47** 10032